Climate Change Scenarios for the California Region

Daniel R. Cayan(1,2), Edwin P. Maurer(3), Michael D. Dettinger(2,1), Mary Tyree(1) and Katharine Hayhoe(4)

1 Scripps Institution of Oceanography, University of California, San Diego
2 U.S. Geological Survey
2 Santa Clara University
4 Department of Geosciences, Texas Tech University

Abstract

To investigate possible future climate changes in California, a set of climate change model simulations was selected and evaluated. From the IPCC Fourth Assessment activities projections, simulations of 21st century climates under a B1 (low emissions) and an A2 (a medium-high emissions) emissions scenarios were evaluated, along with occasional comparisons to the A1fi (high emissions) scenario. The climate models whose simulations were the focus of the present study were from the Parallel Climate Model (PCM1) from NCAR and DOE, and the NOAA Geophysical Fluids Dynamics Laboratory CM2.1 model (GFDL). These emission scenarios and attendant climate simulations are not "predictions," but rather are a purposely diverse set of examples from among the many plausible climate sequences that might affect California in the next century. Temperatures over California warm significantly during the 21st century in each simulation, with temperature increases from approximately +1.5ºC under the lower emissions B1 scenario in the less responsive PCM1 to +4.5ºC in the higher emissions A2

scenario within the more responsive GFDL model. Three of the simulations (all except the B1 scenario in PCM1) exhibit more warming in summer than in winter. In all of the simulations, most precipitation continues to occur in winter, and relatively small (less than ~10%) change in overall precipitation is projected. The California landscape is complex and requires that model information be parsed out onto finer scales than GCMs presently offer. When downscaled to its mountainous terrain, warming has a profound influence on California snow accumulations, with snow losses that increase with warming. Consequently, snow losses are most severe in projections by the more responsive model in response to the highest emissions.

1.0 Introduction

In May 2005, the California Energy Commission (Commission) and the California Environmental Protection Agency (Cal/EPA) commissioned a report describing the potential impacts of 21st Century climate changes on key state resources. Although precise prediction of the future climate is impossible, selected scenarios representative of possible climate changes, targeted regionally on California, were explored much as in previous and ongoing efforts by the Intergovernmental Panel on Climate Change (IPCC) (Houghton et al 2001), an examination of ecological and related changes in California (Field et al. 1999), the U.S. National Climate Change Assessment (National Assessment Synthesis Team, 2001), and the recent United Kingdom Climate Impacts Programme (www.ukcip.org.uk/resources/publications/documents/UKCIP02_briefing.pdf). Because of resource constraints and a tight timeframe during which this report was completed, the present study focused on a small set of climate scenarios.

This work builds upon previous climate model-based studies of possible climate change impacts on various sectors in the California region, including a broad assessment of possible ecological impacts by Field et al (1999); an assessment of a range of potential climate changes on ecosystems, health and economy in California described by Wilson et al. (2003); a study of how a "business-as-usual emissions scenario simulated by a low sensitivity climate model would afftect water resources in the western United States, overviewed by Barnett et al. (2004); and a multisectoral assessment of the difference in impacts arising from high vs. low greenhouse gas (GHG) emission in Hayhoe et al. (2004; hereafter designated H04).

Global and regional climates have already begun changing, probably from accumulating emissions of anthropogenic greenhouse gases. As reported by the WMO (2005), "since the start of the 20th century, the global average surface temperature has risen between 0.6°C and 0.7°C. But this rise has not been continuous. Since 1976, the global average temperature has risen sharply, at 0.18°C per decade. In the northern and southern hemispheres, the 1990s were the warmest decade with an average of 0.38°C and 0.23°C above the 30-year mean, respectively". The 10 warmest years for the earth's surface temperature all occurred after 1990 (Jones and Palutikof 2006) and 2005 was either the the second or first warmest year on record (Jones and Palutikof 2006; Hansen et al. 2006). Much of the warming during the last four decades is attributable to the increasing atmospheric concentrations of GHGs due to human activities (Santer et al. 1996; Tett et al. 1999; Meehl et al. 2003). At the regional scales of California and western North America, signs of changing climate are also evident, in part reflecting the global changes noted above. Over the past 50 years, trends toward warmer winter and spring temperatures (e.g., Cayan et al 2001), smaller fractions of precipitation falling as snow instead of rain (Knowles et al 2006), a decline in spring snow accumulations in lower and middle elevation mountain zones (Mote et al 2005), an advance of snowmelt by 5 to 30 days earlier in the spring (Stewart et al. 2005), and a similar advance in the timing of spring flower blooms (Cayan et al. 2001).

A ongoing effort by the international climate-science community to prepare the Fourth IPCC Climate Change Assessment provided important background and crucial inputs for the studies reported here. In particular, that international assessment prompted and provided (through the Lawrence Livermore Laboratory Program for Climate Model

Diagnosis and Intercomparison) a large number of climate model simulations of climates under selected GHG emission scenarios. The present effort has focused on a few of the IPCC simulations in order to provide concrete examples of possible impacts and has analyzed the large ensemble of projections generated for the IPCC assessment more cursorily for perspectives on the scenarios selected for intense study in terms of two major sources of climate-change uncertainty: our incomplete understanding of how the climate system responds (as represented by differences between different climate models) and the unknowable future of emissions of GHGs and other contaminants to the atmosphere (as represented by the emissions scenarios considered here).

This paper describes, from California's perspective, the selection of climate models, emission scenarios, and downscaling methods used in the overall study. In particular, it examines differences among projections, and among historical to projected climates in the selected projections as well as in the IPCC4 ensemble of projections as a whole.

2.0 Scenarios and Models

The climate models considered in this effort were amongst those that were prepared and evaluated by the IPCC, as described, for example, in the IPCC Third Assessment (Cubasch et al. 2001), and as being used in the ongoing IPCC Fourth Assessment. A discussion of projections of climate change by climate models is presented by Cubasch, Meehl, et al. (2001) as part of the Third IPCC Climate Change Assessment. For this study, primary criteria for model selection were that the ocean and atmosphere components be freely coupled, i.e., not requiring or using flux-correcting

formulations, and that the models have an atmospheric grid spacing of 250 km or less. Another criteria for model selection was the availability of daily output data.

Models selected for attention here also were required to produce a realistic simulation of aspects of California's recent historical climate— particularly the distribution of monthly temperatures and the strong seasonal cycle of precipitation that exists in the region. In addition, models selected were required to contain realistic representations of some regional features, such as the spatial structure of precipitation. Because the observed California climate has exhibited a considerable of natural variability at seasonal to interdecadal time scales, the historical simulations by the climate models were required to include realistic variability at these time scales.

Finally, the selection of models was designed to include models with differing levels of sensitivity to GHG forcing. All these criteria, taken together, identified two global climate models (GCMs), the Parallel Climate Model (PCM; with simulations from NCAR and DOE groups; see Washington et al. 2000; Meehl et al. 2003) and the NOAA Geophysical Fluid Dynamics Laboratory (GFDL) CM2.1 model (Stouffer et al. 2005; Delworth et al. 2006; Knutson et al. 2005). In some parts of California's assessment activities, the UK Hadley Center HadCM3 model (Gordon et al. 2000; Pope et al. 2000) was also used; the simulations by that model were described in, and derived from, the H04 study.

The choice of GHG emissions scenarios focused on herein, A2 (medium-high) and B1 (low) emissions, was based upon implementation decisions made earlier by IPCC4 (Nakic'enovic' et al. 2000), and on availability of certain crucial outputs that varied from emissions scenario to scenario. In addition to the two scenarios primarily

addressed herein, results from H04 based on a third scenario, A1fi (high emissions), was also used in some part of the overall assessment. These A1fi results are compared with selected results in the present study.

The B1 scenario assumes that global (including California) CO_2 emissions peak at approximately 10 gigatons per year (Gt/yr) in mid-21st century before dropping below current levels by 2100. This yields a doubling of CO_2 concentrations relative to its pre-industrial level by the end of the century, followed by a leveling of the concentrations (Fig. 1). Under the A2 scenario, CO_2 emissions continue to climb throughout the century, reaching almost 30 Gt/yr. By the end of the 21st century, CO_2 concentrations reach more than triple their pre-industrial levels. The A1fi scenario has high emissions until about 2080, when they finally by Century's end. The emissions result in CO_2 concentrations that reach about 950 ppm in 2100.

Both the GFDL and PCM modeling groups performed historical simulations--under the so-called 20C3M conditions (see http://www-pcmdi.llnl.gov/projects/cmip/ann_20c3m.php), that allow us to compare global climate model performance to historical observations during late-19th and entire-20th Centuries. 20C3M runs for GFDL span 1861-2000 and for PCM span 1890-1999. The 20C3M conditions used in both models accounted for historical inputs into the atmosphere of aerosols from volcanic eruptions, changes in solar irradiance, and anthropogenic GHG and aerosol loadings (Delworth et al., 2006; Meehl et al., 2003). The 1961-1990 period of modeled climate was used in the present study as a climatology, a benchmark to which future-climate simulations were compared.

3.0 Climate Model Simulations: a California Perspective

Most of the impacts considered in the California assessment are driven by changes in climate at the surface, so we focus on characteristics related to surface air temperature and precipitation in the region.

3.1 Temperature projections

Each of the model projections contains symptoms of global climate change over the California region. As we know from previous studies (.e.g, H04, Dettinger 2005), there is more consistency in the changes of some elements, such as temperature, than others, such as precipitation. Due to differences in the two models' parameterizations, sensitivities and responses to greenhouse gases and other forcings, there are substantial differences between the projections by the two models. PCM has relatively low sensitivity of global and regional temperature to GHG forcing and the GFDL model has a relatively high sensitivity, compared to the larger set of IPCC global climate models (Cayan et al. 2006). There also are significant differences between the two GHG emission scenarios that grow over time, an aspect of this problem that has been emphasized in previous studies (IPCC 2001, H04.) and that is again an important theme in the present results. Northern California temperature warms significantly between 2000 and 2100, with trends ranging from approximately 1.5ºC in the lower emissions B1 scenario within the less responsive PCM model to 4.5ºC in the higher emissions A2 scenario within the more responsive GFDL model (see Table 1). To put this in

perspective, these projected temperature changes over the next century are slightly larger than the differences in annual mean temperature between Monterey and Salinas, and between San Francisco and San Jose, respectively. The difference in annual mean temperatures between Monterey (18.5ºC) and Salinas (19.9ºC) is 1.4ºC and the difference between San Francisco Mission Delores (17.6ºC) and San Jose (21.7ºC) is 4.1ºC.

In both models, warming is greater under the higher emission A2 scenario than under the lower emission B1 scenario. The progress of warming during 21st century is approximately linear in each of the model runs, although there are substantial year to year variations in temperature associated with the normal climate variations on a variety of time scales. Additionally, projected warmings in the A1fi simulations by PCM (H04) were greater than those in the A2 simulations examined here, yielding 3.8ºC warming in A1Fi (Table 1 of H04) compared to 2.7ºC warming in A2, as shown in Table 1. This additional A1fi warming is roughly in proportion to the greater GHG concentrations by end of century in this more extreme scenario. Seasonally, the model projections tend to contain higher amounts of warming in summer than in winter (Figure 2).

In the 30 years from 2005-34, warming--even in PCM under B1--amounts to more than 0.5 C in winter and summer. This near-term warming is sufficient to reduce (increase) substantially the number of cold (warm) temperature outbreaks in summer and winter, effectively eliminating cooler tercile summers already in the GFDL projections. By the 30 year from 2070-99, under all the scenarios considered here (including A1fi from H04,) northern California summer temperatures increase in GFDL projections by 6.4ºC under A2 and 3.6ºC under B1. In the last parts of the 21st Century, counts of seasonal temperatures falling into the lower and upper terciles, for a northern California

location, reveals a remarkable change (Fig. 3). By 2070-2099, in all of the model runs (except PCM B1), seasonal mean temperatures in the lower third of the historical distribution have been eliminated, and in the PM B1 projection, no more than two winters and one summer being is that cool in any decade. Also, the warming greatly reduces the number of seasonal temperatures in the middle tercile, at the expense of large, almost unanimous, increases into the warmest third of the distribution.

The shift in the distribution of seasonal temperatures is mirrored by a similar shift in daily temperatures. The occurrence of extremely warm daily mean temperatures, exceeding the 99.9 percentile of their historical distributions for the June-September summer months, tallied for the PCM and GFDL A2 simulations (Table 2, upper), increases to 50 - 500 times their historical frequency by 2070-2099. Conversely, the incidence of even moderately cool daily mean winter temperatures decreases markedly (Table 2, lower).

Three of the simulations (all except the PCM B1 projection) yield more warming in summer than in winter. In the high emission A2 projections for northern California, mean temperatures increase by the end of the 21st century by 2.6ºC and 5.3ºC in summer and 2.4ºC and 3.3ºC in winter, in the PCM and GFDL models respectively. If the projected summer amplification of warming occurs, it has important implications for impacts such as ecosystems, agriculture, water and energy demand, and the occurrence of heat waves, which can have consequences for public health and the economy.

As might be expected from the large thermal capacity of the ocean relative to land, the temperature change at the sea surface along the California coast is less than that above the adjacent land surface. Figure 4 illustrates this effect in the warming that

occurs in summer (June-August) in A2 simulations by GFDL and PCM in a swath from coastal ocean to land. The 2070-2099 warming of surface air increases landward across southern California from 1.8 ºC to 3.2 ºC in PCM and from 2.3 ºC to 5.5 ºC in GFDL.

3.2 Precipitation projections

T he Mediterranean seasonal precipitation regime in California is not projected to change noticeably. This is indicated by the monthly mean precipitation for the B1 and A2 simulations from PCM and GFDL over northern California, southern central California, and southern California in Figure 5. In all simulations, most precipitation over northern California and southern central California continues to occur in winter. In the PCM historical and climate change simulations, climatological precipitation in southern California exhibits a fall peak (notably in the southern part of the state as shown in "southern California" on the bottom panels of Figure 5), which is not in agreement with the strong winter season Mediterranean precipitation regime observed there. Summer precipitation changes only incrementally, and actually decreases in some of the simulations, so there is no simulated consensus of a stronger thunderstorm activity.

The projections from both models were characterized by relatively modest trends in mean precipitation during the 2000-2100 period (Table 1). In Northern California, by end of century, projected precipitation increases slightly or does not change in one model (PCM), and decreases by 10- 20% in the other model (GFDL). Analysis of California precipitation changes produced under B1 and A2 emissions scenarios in 11 global climate models by Maurer (2005) also finds only modest changes in annual precipitation, but an increase in precipitation in winter months, but a decrease in spring months; our analyses

of the larger set of IPCC model runs has hints of these seasonal tendencies, but only marginally. The small annual precipitation changes are consistent with the fact that although, in general, under global warming, global rates of precipitation are projected to increase, these increases tend to be geographically focused in the tropics and higher latitude extra-tropics. In most current projections of global warming, subtropical and lower middle latitude regions exhibit little change in precipitation and in some cases become drier.

Although little change (often in the form of small decreases) in northern Californian precipitation is projected during the 21st Century, there is a modest tendency for increases in the numbers and magnitudes of large precipitation events, illustrated in Table 3 by the number of daily precipitation events falling into the 99.0 and 99.9 percentiles compared to the corresponding frequencies in the historical-period simulations from the same GCMs.

Similar to observations, precipitation in the projections exhibits considerable monthly to interdecadal variability. The anomalous atmospheric circulation patterns in the simulations that produce much of the precipitation variability are quite similar to those in nature. Winter season precipitation is mostly derived from North Pacific winter storms, as demonstrated by comparing the correlations between Northern California monthly precipitation and 500 HPa height (500 millibar height), mapped over the Pacific and western North America domain for the 1960-91 and 2070-2099 periods from the A2 simulations of GFDL and PCM, to the correlation in observations (Fig. 6). The models also exhibit a significant El Nino/Southern Oscillation signal from interannual sea surface temperature (SST) variations in the tropical NINO 3.4 region (Cayan et al. 2006). These

SST variations are teleconnected to anomalous storm activity in the North Pacific and western North America storm activity, with the warm (El Nino) phase favoring a wetter pattern in southern California and the Southwest and the cool (La Nina) phase favoring drier conditions there (e.g. Dettinger et al. 1998). The models, to a greater or lesser degree replicate this pattern, illustrated in Figure 7. In the model projections of 21st Century climate, the frequency of warm tropical events (El Niños) remains about the same as in the historical simulations, and model El Niño events continue to be related to anomalous precipitation patterns over California.

Simulated interannual-to-interdecadal variability of precipitation and temperature is prominent and does not change appreciably from the historical period of the simulations to the 21st Century. This is evident from plots of ensembles of the same model and same scenario, simply run in perturbed fashion using different initial conditions (Fig. 8). This nontrending, shorter period variability is important because large impacts are most likely to occur secular changes are superimposed on (generally larger) short period variations to cause extreme phenomena such as floods, drought, and heat waves. An ensemble of simulations, accomplished by seeding the model simulations with differing initial conditions, for historical conditions and for a given GHG emission scenario, provides a measure of the internal variability of a particular climate model. The intra-scenario variability for the two models is fairly high, as seen in the set of historical and climate change simulations of annual precipitation in Figure 8. Similar variability, albeit superimposed on a rising trend, are exhibited by a set of ensembles of winter and summer temperature from the PCM A2 simulation (not shown). The projected trends

occur in the context of the seemingly unaltered occurrence of this (simulated) natural variability.

To put the two scenarios and the two GCMs, that are the focus of this assessment, into broader perspective, it is useful to compare them with projections of climate changes over California from the larger collection of simulations. Following an analysis by Dettinger (2005*, 2006*), projection distributions were estimated for a much larger subset of the Fourth IPCC Assessment simulations, including 84 simulations from a total of 12 different climate models responding to three different emission scenarios: higher (A1b), middle-high (A2), and low (B1). This large ensemble of simulations describes a range of projected temperature anomalies in the 2070-99 period, all positive, from relatively modest to quite large (e.g., from about +2ºC to +7ºC). The distribution of precipitation totals includes both positive and negative anomalies that cluster with moderate change around present-day averages and with modest increases in the range of precipitation variability and differences within the ensemble, shown in Table 1 and in univariate (Figure 9) and joint (Figure 10) distributions of temperature and precipitation.

Throughout the 100 year simulation, Northern California conditions projected by PCM remain in the lower half of the temperature distributions, exhibiting a relatively modest degree of warming. The small changes experienced by PCM B1 and A2 are close to the center of the overall precipitation distributions. In contrast, Figures 9 and 10 shows that California temperatures projected by GFDL and HadCM3 (from H04) are in the warmer half of the overall temperature distributions. GFDL and HadCM3 projections of precipitation tend to be in the drier parts of the precipitation distributions. The projected precipitation changes are not correlated with the temperature changes

overall, as shown by the joint probability of temperature and precipitation changes in Figure 10. If they were, then warming-moistening or warming-drying trends might be become systematic parts of the projection ensemble. If they were a feature of the IPCC4 projections, such combinations of trends would certainly influence the kinds of snowmelt and streamflow responses that follow. Because these combination occur only randomly in the ensemble, projected precipitation changes (such as they are) and temperature changes are almost independent from model to model, and snowmelt processes must be assessed projection by projection.

4. Reductions in snow accumulation

The selection of GCMs for this study required that they exhibit, on a broad spatial scale, seasonal patterns of simulated precipitation and temperature for the historic period that resemble those in nature. However, many climate impacts arise from finer-grained phenomena, often influenced by topographic features, e.g., notably, the winter and spring snow accumulation in California, which occurs primarily in mountain catchments. Also, even the best models display biases on regional scales that are large enough that the impacts of climate change may be difficult to trace from large-scales to the scales of landscapes and watersheds.

To correct systematic bias in the models and to interpolate the climate changes to scales comparable with topography and landscape, in this study, we employed a statistical bias correction technique and downscaling technique originally developed by Wood et al. (2002) for using global model forecast output for long-range streamflow forecasting. This technique was later adopted to downscale GCM output for use in studies examining the

hydrologic impacts of climate change (H04; Maurer and Duffy, 2005; Payne et al., 2004; Vanrheenen et al., 2004). This is an empirical statistical technique that maps GCM precipitation and temperature during a historical period (1950–1999 for this study) to the concurrent historical observed record, which for this study is taken to be a gridded National Climatic Data Center Cooperative Observer station data set (Maurer et al., 2002). This observed data set, developed at a spatial scale of 1/8º (about 7 miles or 12km), was aggregated to a 2° latitude-longitude spatial resolution.

The combined bias correction/spatial downscaling method used in this study has been shown to compare favorably to different statistical and dynamic downscaling techniques (Wood et al., 2004) in the context of hydrologic impact studies. For precipitation and temperature, cumulative distribution functions (CDFs) are built for each of 12 months for each of the 2° grid cells for both the gridded observations and each GCM (first interpolating raw GCM data onto a common 2º grid) for the historical period (1950–1999). GCM quantiles are then mapped onto the climatological CDF for the entire simulation period. For example, if precipitation at one grid point from the GCM has a value in January of 2050 equal to the median GCM value (for January) for 1950–1999, it is transformed to the median value of the January observations for 1950–1999. For temperature, the linear trend is removed prior to this bias correction step, and is replaced afterward, to avoid increasing sampling at the tails of the CDF as temperatures rise. Thus, the probability distributions of the observations are reproduced by the bias corrected climate model data for the overlapping historical period, while both the mean and variability of future climate can evolve according to GCM projections.

The GFDL model has a resolution (of the atmospheric component) of 2.5º longitude by 2.0º latitude (approximately 137 mi X 137 mi (220 km x 220 km) per grid cell), and the PCM uses a standard T42 resolution (approximately 2.8º, or 155 miles X 186 miles (250 km x 300 km) in California). The spatial scale of the GCMs is very large compared to the scale of interest for many impact studies. For example, the area of one GCM atmospheric grid cell (simulated essentially as one area of constant elevation and land surface condition) is more than 10 times as large as the entire American River basin upstream of Folsom Dam. The Wood et al. (2002) statistical method interpolates the bias corrected GCM anomalies, expressed as a scale factor (for precipitation) and shift (for temperature) relative to the climatological period at each 2° GCM grid cell to the centers of 1/8 degree grid cells over California. These factors are then applied to the 1/8 degree gridded historical precipitation and temperature (examples shown in H04 and Cayan et al. 2006). .

To generate supplemental meteorological data that drives snow accumulation (such as radiative forcing, humidity, etc.) as well as to derive land surface hydrological variables consistent with the downscaled forcing data, the variable infiltration capacity (VIC) model (Liang et al., 1994; Liang et al., 1996) was used. VIC is a macroscale, distributed, physically based hydrologic model that balances both surface energy and water over a grid mesh, and has been successfully applied at resolutions ranging from a fraction of a degree to several degrees latitude by longitude. The VIC model includes a "mosaic" land surface scheme, allowing a statistical representation of the sub-grid scale spatial variability in topography and vegetation/land cover. This is especially important when simulating the hydrologic response in complex terrain and in snow dominated

regions. To account for subgrid variability in infiltration, the VIC model uses a scheme based on work by Zhao et al. (1980). The VIC model also features a nonlinear mechanism for simulating slow (baseflow) runoff response, and explicit treatment of a vegetation canopy on the surface energy balance. Following the simulation of the water and energy budgets by the VIC model, a second program is used to route the derived runoff through a defined river system to obtain streamflow at specified points. The algorithm used in this study, developed by Lohmann et al. (1996), has since its development been employed in all simulations of streamflow using output from the VIC model. The VIC model has been successfully applied in many settings, from global to river basin scale (Abdulla et al., 1996; Maurer et al., 2001; Maurer et al., 2002; Nijssen et al., 1997; Nijssen et al., 2001), as well as in several studies of hydrologic impacts of climate change (Christensen et al., 2004; H04; Maurer and Duffy, 2005; Payne et al., 2004; Wood et al., 2004). For this study, the model was run at a 1/8-degree resolution (measuring about 150 km^2 per grid cell) over the entire California domain, including all land surface area between latitudes 32ºN and 44ºN and west of longitude 113ºW. For deriving streamflows within the Sacramento-San Joaquin river basin the identical parameterization to VanRheenen et al. (2004) was used.

Although precipitation trends only modestly during the period of the climate simulations, climate warming is projected to reduce snow accumulation in California. This is because warming causes more of the precipitation to fall as rain and less as snow (Knowles et al. 2006). Such changes in precipitation form (more rain and less snow) are indicated by substantial changes in daily temperature during days with precipitation, shown in Figure 12 for Northern California projections. Notably, minimum temperatures

tend to be warmest during days with the heaviest precipitation. For each model and each emission scenario, all precipitation categories, including dry days, are warmer in 2070-99 than the historical climatological distribution, with wetter days generally warming more than dry days.

During the historical period, snow accumulation has already exhibited losses of order 10% of April 1 snow water equivalent (SWE) across the western conterminous United States (Mote et al 2005), and is expected to melt earlier as climate warming continues (Knowles and Cayan 2002; Wood et al. 2004; Maurer and Duffy 2005). Each of the climate simulations, when used as input to the VIC hydrologic model, yields substantial losses of spring snow accumulation over the Sierra Nevada. These losses become progressively larger as warming increases during the 21st Century. The losses are also largest in projected responses to the simulated climates from the more sensitive model under the highest GHG emissions. As depicted in Table 4, and Figures 13 and 14, the losses (negative) or gains (positive) of April 1 snow water equivalent (SWE) in the San Joaquin, Sacramento and Trinity drainages, as percentages of (1961-1990) historical averages, range from +6% to -29% (for the 2005-2034 period), from -12% to -42% (for 2035-64), and from -32% to -79% (for the 2070-99 period). The GFDL model, with its greater temperature sensitivity to increased GHG concentrations, produces snowpack losses about twice as large as those produced by the PCM. Most but not all of this difference can be ascribed directly to the projected warmings.; the remainder is mostly due to the declining precipitation totals that GFDL projects. For both models, snowpack losses are greatest in the warmer, more GHG-emitting (A2) scenario. By 2070-2099, virtually no snow is left below 1000 m under this scenario. In terms of water storage

volume, snow losses have greatest impact in relatively warm low-middle and middle elevations between about1000 and 2000m, with losses of 60% to 93% and between about 2000m and 3000m, with losses of 25% to 79%. Because the highest elevations in the Sierra Nevada tend to be in the southern part of the range, the largest reductions in snow accumulation occur in the central and northern parts of the range (Figure 14).

5. Discussion and Summary

A purposely diverse set of possible 21st Century climates for California were investigated to provide the context and drivers for an evaluation of possible drivers and impacts in a variety of sectors. The first-order surface climate variables, temperature and precipitation—and some immediate implications for snowpacks and runoff in the State, were the focus of the present study. The projections analyzed were based strictly on simulations by *global* climate models. Although regional models will be needed to distribute climate over the complex landscape of California, the first-order climate changes tend to derive from the large, indeed global, scale responses to increasing GHGs, even when considered at the California scale.

These projections that were the focus of the current study are the responses of mostly from two state-of-the-art global climate models forced (mostly) by two GHG emission scenarios. These projections are not "predictions," but rather represent purposely diverse examples from among the many plausible climates that may occur in the 21st Century. Future GHG concentrations are uncertain because they depend on future social, political, and technological decisions, and thus the IPCC has produced four "families" of emission scenarios (IPCC, 2001). To explore some of the range of futures

expressed by the IPCC emissions scenarios, an A2 emissions scenario (with its medium-high emissions) and a B1 (low emissions) scenario were selected from the current IPCC Fourth climate-assessment archives for evaluation. The global climate model simulations focused upon here were from the NCAR/DOE group's PCM1 model and GFDL's CM2.1 Among these and all other IPCC projections, temperatures are projected to rise significantly during the 21st century. The magnitude of projected warming varies from model to model, and emission scenario to emission scenario. California's temperatures rise, between 2000 and 2100, by 1.7°C to 3.0°C in the lower range of projected warmings, 3.1°C to 4.3°C in the medium range, and 4.4°C to 5.8°C in the high range. Warming affects both wet and dry days to about the same degree. During the 2070-2099 period, the least warming projected would be equivalent to moving from Monterey to Salinas and the largest warming would be like moving from San Francisco to San Jose.

Another way to think about these warming trends is in terms of the marked shifts they produce in the lower, middle and upper terciles of historical temperature distributions. By 2070-2099, in all of the projections, temperature increases were sufficient to nearly eliminate seasonal mean temperatures in the lower (historical) tercile and sharply reduce those in the middle (historical) tercile. Such climate changes would be, in the words of Hansen et al 2006 , " climate changes outside of the range of local experience". A noteworthy feature in the temperature projections is that the warming through the 21st Century does not level off, especially in projections using the medium and high greenhouse gas emission scenarios, implying that California's climate would continue to warm in (at least) the subsequent decades of the 22nd Century.

There is no consensus trend among the precipitation projections for California during the next century. Instead, the large majority of the recent IPCC model projections, including several simulations that not analyzed in detail here, yield relatively small (5-20%) change in total precipitation. It is worth emphasizing though, that a 10%-20% change in annual precipitation is *not* a minor gain or loss. In the historical record, a 15% loss in precipitation is sufficient to cast a year into the lowest third of the annual totals, and, since runoff is a non-linear outcome of precipitation, lessening the supply in many cases drives runoff disproportionately lower.

Continued warming in California will have uneven effects on the California landscape. For example, warming will diminish snow accumulations, of resulting trends toward more rain and less snow, and earlier snowmelt, especially in lower to middle elevations of mountain catchments. Losses of snow, perhaps the early signs of climate change, are already being observed in the western United States, and hydrologic simulations indicate that the losses will increase as the warming increases. In the present study, the most severe losses are produced by the more sensitive CM2.1 model under the higher A2 (and A1fi) emissions. By 2070-99, under the A2 and B1 emission scenarios in the PCM and GFDL models, losses of snow water equivalent (SWE) in the San Joaquin, Sacramento and Trinity drainages, as percentages of (1961-1990) historical averages, range from -32% to -79%. By 2070-2099, virtually no snow is left below 1000m under the A2 scenario in the GFDL model. Because higher elevation, and thus cooler, areas in the Sierra Nevada are mostly in the southern part of the range, the largest reductions in snow are projected to occur in the central and northern range.

Acknowledgments Support for DC, EM, MT and KH was provided by the State of California through the California Energy Commission PIER Program and the California Environmental Protection Agency. DC and MT were also supported by NOAA RISA Program through the California Applications Center and from DOE. MD's and DC's involvement were facilitated by the USGS Priority Ecosystems Study of the San Francisco Estuary.

References

Abdulla, F. A., D. P. Lettenmaier, E. F. Wood, and J. A. Smith, 1996: Application of a macroscale hydrologic model to estimate the water balance of the Arkansas-Red River basin. *J. Geophysical Research*, ***101***, 7449-7459.

Barnett, T., R. Malone, W. Pennell, D. Stammer, A. Semtner, and W. Washington, 2004: The effects of climate change on water resources in the west: Introduction and Overview. Climatic Change, **62**, 1-11.

Cayan, D.R., S. Kammerdiener, M. D.Dettinger, J. M. Caprio, and D. H. Peterson, 2001: Changes in the onset of spring in the western United States. *Bull. Am. Met Soc*., **82**(3), 399-415.

Cayan, D.C, Maurer, E., Dettinger, M.D., Tyree, M. Hayhoe, K. Bonfils, C., Duffy, P., and B. Santer **,** 2006: Climate Scenarios for California. FINAL white paper from California Climate Change Center, publication # CEC-500-2005-203-SF, posted: March 15, 2006. http://www.climatechange.ca.gov/climate_action_team/reports/index.html

Christensen, N. S., A. W. Wood, N. Voisin, D. P. Lettenmaier, and R. N. Palmer, 2004: The effects of climate change on the hydrology and water resources of the Colorado River basin. *Climatic Change*, ***62***, 337-363.

Cubasch, U., Meehl, G.A., Boer, G.J., Stouffer, R.J., Dix, M., Noda, A., **Senior, C.A.**, Raper, S. and Yap, K.S., 2001: Projections of future climate change. In 'Climate Change 2001: The scientific basis'. J. T. Houghton, Ding Yihui and M. Noguer (Eds), Cambridge University Press.

Delworth, T. et al., 2006: GFDL's CM2 global coupled climate models - Part 1: Formulation and simulation characteristics. *J. Climate*, 19(5), 643-674.

Dettinger, M.D., 2005a: From climate-change spaghetti to climate-change distributions for 21st Century California. San Francisco Estuary and Watershed Science, **3**(1), http://repositories.cdlib.org/jmie/sfews/vol3/iss1/art4 .

Dettinger, M.D., 2005b: A component-resampling approach for estimating probability distributions from small forecast ensembles. Climatic Change, 31 p. (*in press*).

Dettinger, M.D., Battisti, D.S., Garreaud, R.D., McCabe, G.J., and Bitz, C.M., 2001: *Interhemispheric effects of interannual and decadal ENSO-like climate variations on the Americas*, in V. Markgraf (ed.), Interhemispheric climate linkages: Present and Past Climates in the Americas and their Societal Effects. Academic Press, 1-16.

Field, C. B., Daily, G. C., Davis, F. W., Gaines, S., Matson, P. A., Melack, J. & Miller, N. L. , 1999: *Confronting Climate Change in California: Ecological Impacts on the Golden State.* Union of Concerned Scientists, Cambridge, MA, and Ecological Society of America, Washington, DC.

Gordon, C., Cooper, C., Senior, C. A., Banks, H., Gregory, J. M., Johns, T. C.,Mitchell, J. F. B. and Wood, R. A., 2000: The simulation of SST, sea ice extents and ocean heat transports in a version of the Hadley Centre coupled model without flux adjustments. *Clim. Dyn.* **16,** 147–168.

Hanemann, L. S. Kalkstein, J. Lenihan, C. K. Lunch, R. P. Neilson, S. C. Sheridan, and J. H. Verville, 2004: Emissions pathways, climate change, and impacts on California. *Proceedings of the National Academy of Sciences of the United States of America*, **101**, 12422-12427.

Hansen, J. Ruedy, R., Sato, M. and K. Lo, 2006: GISS Surface Temperature Analysis: Global Temperature Trends: 2005 Summation. http://data.giss.nasa.gov/gistemp/2005/

Hansen, J., Mki. Sato, R. Ruedy, L. Nazarenko, A. Lacis, K. Lo, G.A. Schmidt, G. Russell, I. Aleinov, M. Bauer, S. Bauer, E. Baum, N. Bell, B. Cairns, V. Canuto, M. Chandler, Y. Cheng, A. Cohen, A. Del Geno, G. Faluvegi, E. Fleming, A. Friend, T. Hall, C. Jackman, J. Jonas, M. Kelley, N. Kiang, D. Koch, G. Labow, J. Lerner, S. Menon, R.L. Miller, T. Novakov, V. Oinas, Ja. Perlwitz, Ju. Perlwitz, D. Rind, A. Romanou, D. Shindell, P. Stone, S. Sun, D. Streets, N. Tausnev, D. Thresher, M. Yao, and S. Zhang 2005. Dangerous human-made interference with climate: A GISS modelE study. *J. Geophys. Res.*, submitted

Hayhoe, K., D. Cayan, C. B. Field, P. C. Frumhoff, E. P. Maurer, N. L. Miller, S. C. Moser, S. H. Schneider, K. N. Cahill, E. E. Cleland, L. Dale, R. Drapek, R. M. ,2004: Emissions pathways, climate change, and impacts on California. PNAS **101**(34):12422-12427, 24 August 2004.

Hegerl, G.C., H. von Storch, K. Hasselmann, B.D. Santer, U. Cubasch, P.D. Jones, 1996: Detecting Greenhouse-Gas-Induced Climate Change with an Optimal Fingerprint Method. *J. Climate* **9**(10), 2281-2306.

Houghton, J. T., et al., (eds.), 2001: The scientific basis: Contribution of Working Group I to the Third Assessment Report of the Intergovernmental Panel on Climate Change. Climate Change, Cambridge University Press, 525–582.

Jones, P. and P. Palutikof, 2006: Global Temperature Record. Climate Research Unit, University of East Anglia. http://www.cru.uea.ac.uk/cru/info/warming/

Knowles, N. & Cayan, D. R., 2002: Potential effects of global warming on the Sacramento/San Joaquin watershed and the San Francisco estuary. *Geophys. Res. Lett.* **29**(18)**,** 1891–1895.

Knowles, N., M.D. Dettinger and D.R. Cayan, 2006: Trends in Snowfall versus Rainfall in the Western United States. *J. Climate*, in press.

Knutson, et al., 2005: Assessment of Twentieth Century Regional Surface Temperature Trends using the GFDL CM2 Coupled Models. *J. Climate*, Sept. 2005, (*accepted*).

Lettenmaier, D. P., and T. Y. Gan, 1990: Hydrologic Sensitivities of the Sacramento-San Joaquin River Basin, California, to Global Warming, edited. Water Resources Research, pp. 69-86.

Liang, X., D. P. Lettenmaier, E. Wood, and S. J. Burges, 1994: A simple hydrologically based model of land surface water and energy fluxes for general circulation models. *J. Geophysical Research*, **99**(D7), 14,415-414, 428.

Liang, X., D. P. Lettenmaier, and E. F. Wood, 1996: One-dimensional statistical dynamic representation of subgrid spatial variability of precipitation in the two-layer variable infiltration capacity model. *J. Geophysical Research*, **101**(D16), 21, 403-421, 422.

Lohmann, D., R. Nolte-Holube, and E. Raschke, 1996: A large-scale horizontal routing model to be coupled to land surface parameterization schemes. *Tellus*, **48A**, 708-721.

Maurer, E.P., 2005, Uncertainty in hydrologic impacts of climate change in the Sierra Nevada Mountains, California under two emissions scenarios, *Climatic Change* (in review).

Maurer, E. P., and P. B. Duffy, 2005: Uncertainty in projections of streamflow changes due to climate change in California, *Geophysical Research Letters*, **32**, L03704.

Maurer, E. P., A. W. Wood, J. C. Adam, D. P. Lettenmaier, and B. Nijssen, 2002: A Long-Term Hydrologically-Based Data Set of Land Surface Fluxes and States for the Conterminous United States. *J. Climate*, **15**(22), 3237-3251.

Maurer, E. P., G. M. O'Donnell, D. P. Lettenmaier, and J. O. Roads, 2001: Evaluation of the land surface water budget in NCEP/NCAR and NCEP/DOE reanalyses using an off-line hydrologic model. *J. Geophysical Research*, **106**(D16), 17841-17862.

Meehl, G.A., W.M. Washington, T.M.L. Wigley, J.M. Arblaster and A. Dai, 2003: Solar and Greenhouse Gas Forcing and Climate Response in the Twentieth Century. *J. Climate*, **16**(3), 426-444.

Miller, N. L., K. E. Bashford, and E. Strem, 2003: Potential impacts of climate change on California hydrology. *J. the American Water Resources Association*, **39**, 771-784.

Mote, Philip W., Hamlet, Alan F., Clark, Martyn P., Lettenmaier, Dennis P. Declining mountain snowpack in western North America, 2005:. *Bulletin of the American Meteorological Society*, **86**, 39-49

National Assessment Synthesis Team, 2001: Climate Change Impacts on the United States: *The Potential Consequences of Climate Variability and Change*, US Global Change Research Program**.**

Nakic´enovic´, N., J. Alcamo, G. Davis, B. de Vries, J. Fenhann, S. Gaffin, K. Gregory, A. Gru¨bler, T. Y. Jung, T. Kram, *et al.*, 2000: *Intergovernmental Panel on Climate Change Special Report on Emissions Scenarios.* Cambridge Univ. Press, Cambridge, U.K.

Nijssen, B., D. P. Lettenmaier, X. Liang, S. W. Wetzel, and E. Wood, 1997: Streamflow simulation for continental-scale basins, *Water Resources Research*, **33**, 711-724.

Nijssen, B., G. M. O'Donnell, D. P. Lettenmaier, D. Lohmann, and E. F. Wood, 2001: Predicting the discharge of global rivers. *J. Climate*, **14**(15), 1790-1808.

North G.R. and M.J. Stevens, 1998: Detecting climate signals in the surface temperature record, *J. Climate*, **11**(4), 563-577.

Payne, J. T., A. W. Wood, A. F. Hamlet, R. N. Palmer, and D. P. Lettenmaier, 2004: Mitigating the effects of climate change on the water resources of the Columbia River Basin. *Climatic Change*, **62**, 233-256.

Pope, V. D., Gallani, M. L., Rowntree, P. R.&Stratton, R. A., 2000; The impact of new physical.parameterisations in the Hadley Centre **climate** model – HadAM3. *Clim. Dyn.* **16,** 123–146.

Santer, B. D., T.M.L Wigley, T.P. Barnett, E. Anyamba, 1996: Detection of climate change and attribution of causes. Cambridge University Press, New York, NY (USA).

Stewart, I., Cayan, D.R., and Dettinger, M.D., 2005: Changes towards earlier streamflow timing across western North America. J. Climate 18, 1136-1155.

Stouffer et al, 2005: GFDL's CM2 global coupled climate models - Part 4: Idealized climate response. *J. Climate, (accepted for publication).*

Stott P.A., 2003: Attribution of regional-scale temperature changes to anthropogenic and natural causes. *Geophys. Res. Let.*, **30**(14).

Stott P.A., S.F.B. Tett, G.S. Jones, M.R. Allen, J.F.B. Mitchell and G.J. Jenkins, 2000: External control of 20th century temperature by natural and anthropogenic forcings. Science, **290**, 2133-2137.

Tett, S. F. B., P. A. Stott, M. R. Allen, W. J. Ingram, and J. F.B. Mitchell, 1999: Causes of twentieth century temperature change. *Nature*, **399**, 569-572.

Vanrheenen, N. T., A. W. Wood, R. N. Palmer, and D. P. Lettenmaier, 2004: Potential implications of PCM climate change scenarios for Sacramento-San Joaquin River Basin hydrology and water resources. *Climatic Change*, **62**, 257-281.

Washington, W. M., Weatherly, J. W., Meehl, G. A., Semtner, A. J., Bettge, T. W., Craig, A. P., Strand, W. G., Arblaster, J., Wayland, V. B., James, R. & Zhang, Y., 2000: *Clim. Dyn.* **16**(10/11), 755–774.

Wilson, T., et al., Global Climate Change and California: Potential Implications for Ecosystems, Health, and the Economy. 2003, California Energy Commission: Sacramento. 1*138. Available at http://www.energy.ca.gov/pier/final_project_reports/500-03-058cf.html

Wood, A. W., E. P. Maurer, A. Kumar, and D. P. Lettenmaier, 2002: Long-range experimental hydrologic forecasting for the eastern United States, *J. Geophysical Research-Atmospheres*, **107**(D20), 4429.

Wood, A. W., L. R. Leung, V. Sridhar, and D. P. Lettenmaier, 2004: Hydroloc implications of dynamical and statistical approaches to downscaling climate model outputs. *Climatic Change*, **62**, 189-216.

World Meteorological Organization (WMO), 2005: Statement on the Status of the Global Climate in 2005: Geneva, 15 December, 2005. http://www.wmo.ch/index-en.html

Zhao, R.-J., L.-R. Fang, X.-R. Liu, and Q.-S. Zhang, 1980: The Xinanjiang model, in *Hydrological Forecasting, Proceedings, Oxford Symposium*, edited, pp. 351-356, IAHS Publ. 129.

Table 1. Temperature and Precipitation Changes, GFDL and PCM B1 and A2 simulations, Northern and Southern California. Temperature units are ºC, precipitation in mm. Mean values are provided for historical (1961-1990) period, and changes between successive 30year periods are shown in subsequent columns for the models/emission scenarios, as indicated.

				2005-2034				2035-2064				2070-2099			
	Change in Temp and Precip	1961-1990		GFDL		PCM		GFDL		PCM		GFDL		PCM	
		GFDL	PCM	A2	B1	A2	B1	A2	B1	A2	B1	A2	B1	A2	B1
NOCAL	Annual °C	9.3	8.0	1.5	1.4	0.5	0.5	2.3	2.2	1.3	.8	4.5	2.7	2.6	1.5
	Summer °C (JJA)	21.5	17.9	2.1	1.7	0.9	0.6	3.4	2.6	1.7	1.1	6.4	3.7	3.3	1.6
	Winter °C (DJF)	-.46	.08	1.4	1.3	0.1	0.7	1.7	2.1	0.9	2.4	3.4	2.3	2.3	1.7
	Annual mm/%	1098	750	+0.3	+2	-0.4	+7	-3	-2	-2	+3	-18	-9	-2	0
	Summer mm/% (JJA)	14	14	-29	-6	+28	+44	-67	-13	+35	-18	-68	-43	-30	-4
	Winter mm/% (DJF)	649	386	-1	+13	-5	+13	+6	-0.1	-5	-2	-9	-6	+4	+4

				2005-2034				2035-2064				2070-2099			
	Change in Temp and Precip	1961-2000		GFDL		PCM		GFDL		PCM		GFDL		PCM	
		GFDL	PCM	A2	B1	A2	B1	A2	B1	A2	B1	A2	B1	A2	B1
SOCAL	Annual °C	12.2	14.3	1.3	1.3	0.5	0.6	2.3	2.1	1.2	0.8	4.4	2.7	2.5	1.6
	Summer °C (JJA)	23.2	23.4	1.7	1.6	0.4	0.5	3.1	2.3	1.3	0.8	5.3	3.2	2.6	1.5
	Winter °C (DJF)	2.4	5.4	1.0	1.0	0.2	0.7	1.7	1.6	1.0	0.6	3.3	2.0	2.4	1.6
	Annual mm/%	537	342	-6	-2	+7	+18	-2	-11	+7	-2	-26	-22	+8	+7
	Summer mm/% (JJA)	7	5	+49	-13	-7	+6	-60	-50	+35	+33	-44	-63	-11	+2
	Winter mm/% (DJF)	320	187	-0.7	+0.8	+1	+32	+9	-9	+6	-6	-2	-26	+8	-0.8

Table 2. Daily Extreme (99.9th % ile) Temperature Occurrences June-September

	No Cal				**So Cal**			
	PCM		**GFDL**		**PCM**		**GFDL**	
	B1	A2	B1	A2	B1	A2	B1	A2
1961-1990	5	5	5	5	5	5	5	5

2005-2034	15	39	53	111	1466	1384	198	195
2035-2064	43	80	165	227	1581	1790	306	496
2070-2099	56	258	210	856	1960	2506	474	1038

Table 3. Daily Extreme Precipitation Occurrences, PCM and GFDL A2 simulations

	No Cal				**So Cal**			
	PCM		**GFDL**		**PCM**		**GFDL**	
	99 % ile	*99.9 % ile*	*99 % ile*	*99.9 % ile*	*99 % ile*	*99.9 % ile*	*99 % ile*	*99.9 % ile*
1961-1990	111	12	111	12	111	12	111	12
2005-2034	117	8	129	19	129	19	93	12
2035-2064	129	14	130	40	130	40	129	7
2070-2099	161	25	127	30	127	30	98	10

Table 4. Change in April 1 snow accumulation, San Joaquin, Sacramento, and parts of Trinity drainages from VIC hydrologic model. Similar computations for HadCM3 A1fi and B1 simulations and for PCM A1fi simulation are presented in Table 1 of Hayhoe et al., 2004.

		2005-2034				2035-2064				2070-2099			
Change in April snowpack SWE	1961-1990	PCM		GFDL		PCM		GFDL		PCM		GFDL	
	PCM	B1	A2	B1	A2	B1	A2	B1	A2	B1	A2	B1	A2
1000-2000 m elevation %	4.0 km^3	-.13	-.35	-.2	-.48	-.26	-.52	-.68	-.61	-.60	-.76	-.75	-.93
2000-3000 m elevation %	6.5 km^3	+.12	-.09	-.04	-.33	-.08	-.21	-.36	-.32	-.25	-.34	-.56	-.79
3000-4000 m elevation %	2.49 km^3	+.19	+.01	+.04	-.13	-.02	-.05	-.16	-.11	-.05	-.02	-..41	-.55
All elevations %	13.0 km^3	+.06	-.15	-.07	-.29	-.12	-.27	-.42	-.37	-.32	-.41	-.59	-.79

Figure 1. Projected atmospheric CO2 concentrations under several of the IPCC emission scenarios.

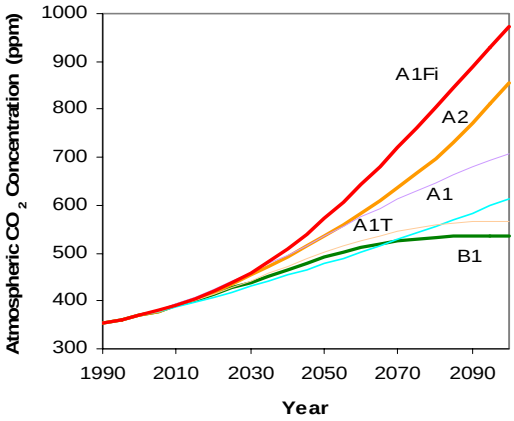

Figure 2. Projected changes in monthly-mean temperature,s in northern California during 2070-2099, and relative to 1961-1990, for PCM and GFDL B1 and A2 simulations.

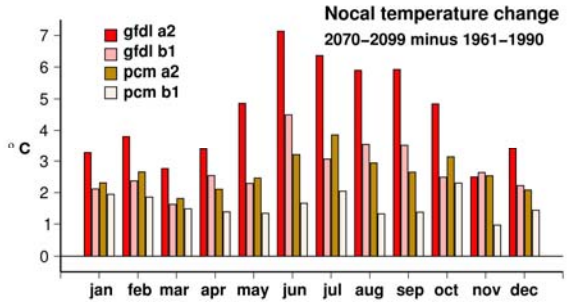

Figure 3. Occurrence of seasonal temperatures falling into coolest (blue) and warmest (red) thirds of their historical (1961-90) distribution for PCM and GFDL simulations, under A2 and B1 emission scenarios. Values plotted are counts in 10-year moving windows with the bars centered in each window.

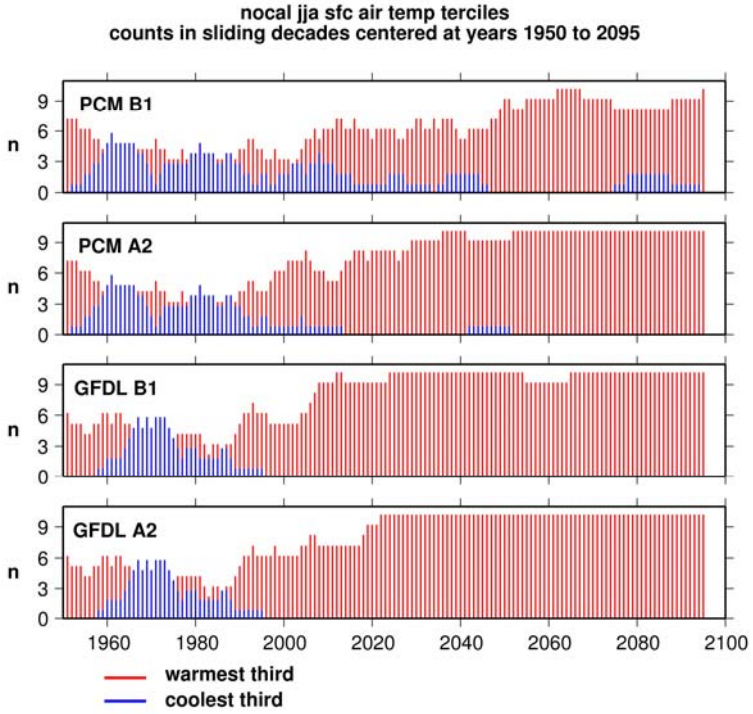

Figure 4. Change in June-August temperatures (2070-2099 minus 1961-1990) for PCM and GFDL A2 simulations along a transect of grid points (shown in inset) from the offshore ocean and to interior land in Southern California.

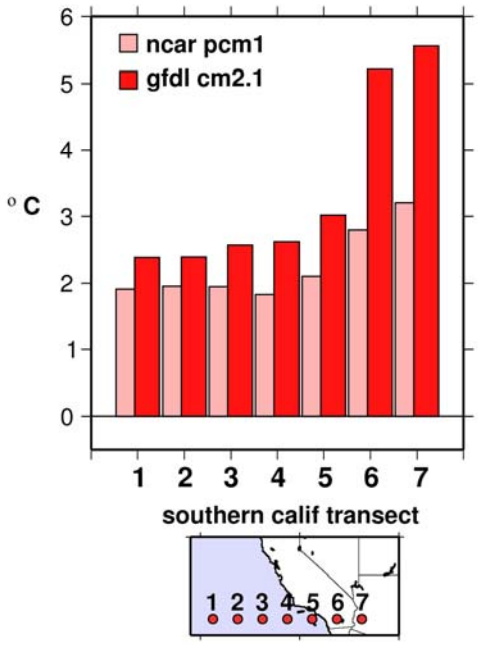

Figure 5. Historical (1961-1990, left) observed and simulated precipitation, and projected (2070-2099, right) average monthly precipitation, Northern California, south Central California, and Southern California.

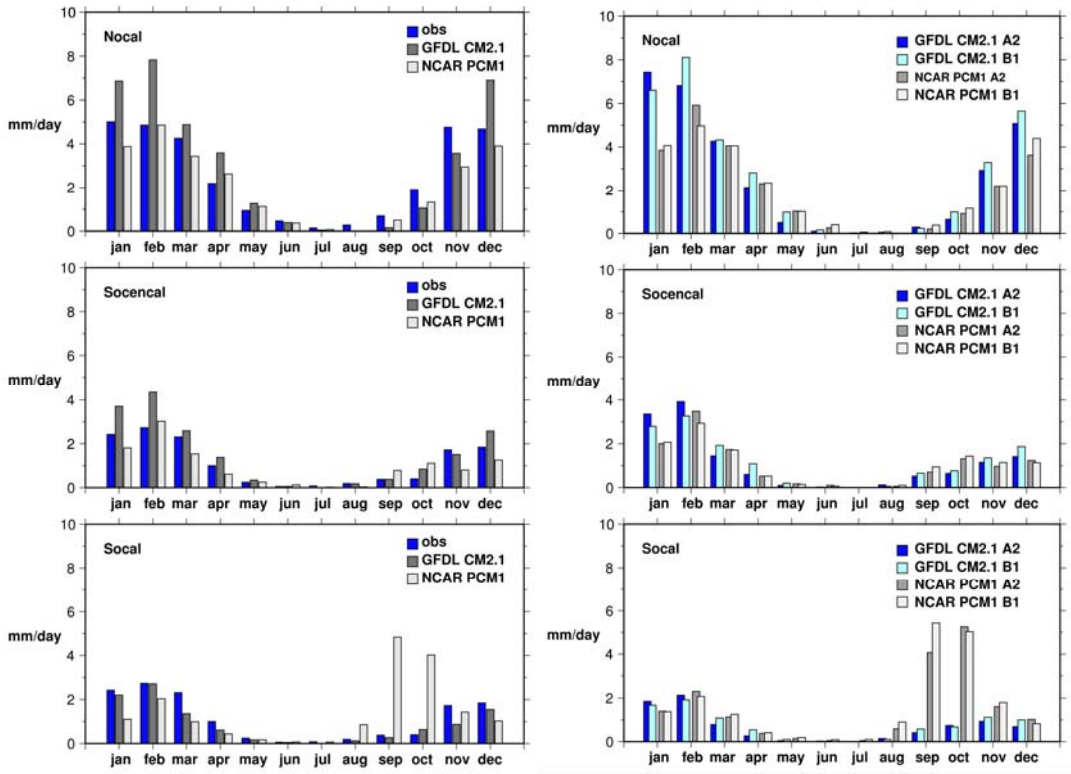

Figure 6. Correlations between Nov-Mar mean precipitation, Northern California, and Nov-Mar 500HPa height anomalies at each point in Pacific-western North America domain for the historical period (1961-1990, left) and for 2070-2099 (right) in GFDL and PCM A2 simulations, and for observations from NCAR/NCEP Reanalysis.

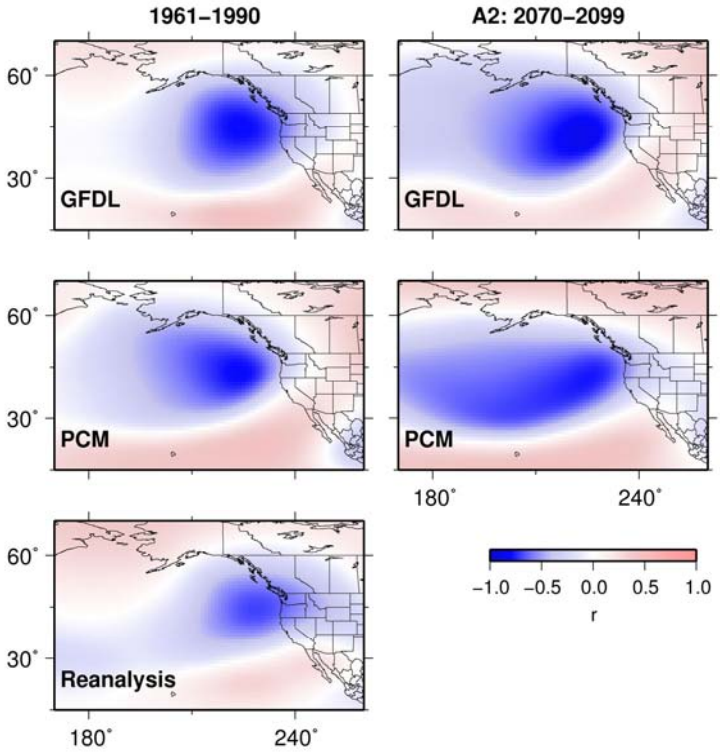

Figure 7. Correlation between Nino 3.4 SST and precipitation across the globe from simulations by GFDL (above) and PCM (middle), along with observations from NCEP/NCAR Reanalysis (www.cdc.noaa.gov/cdc/reanalysis/reanalysis.shtml; below) demonstrate strong connection between tropical Pacific ENSO fluctuations and extratropical precipitation.

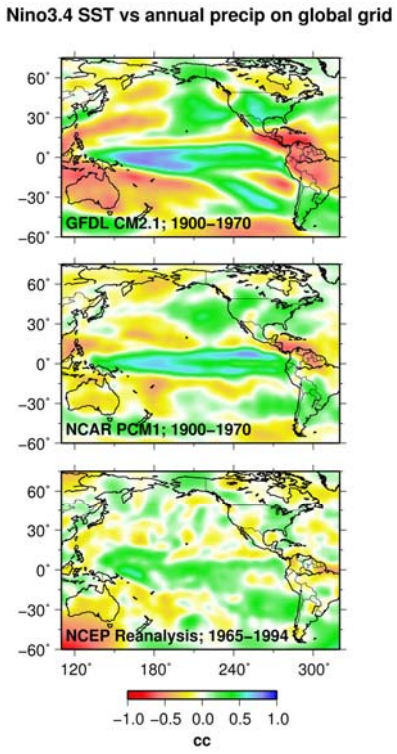

Figure 8. Ensemble of Northern California precipitation projections from multiple simulations by GFDL (top) and PCM (bottom) models under historical and A2 conditions, with the specific runs analyzed herein highlighted.

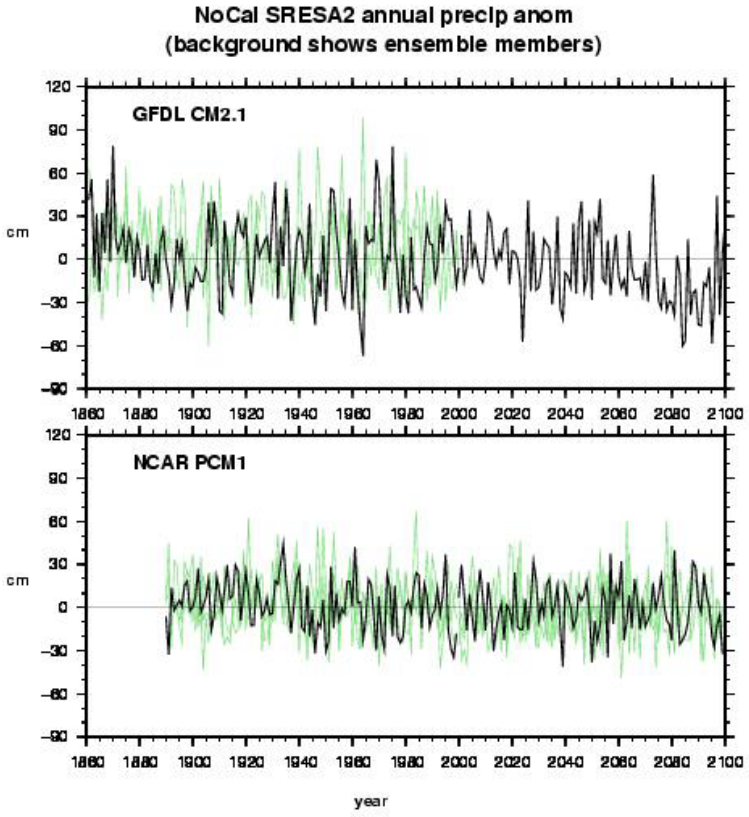

Figure 9. Distribution of anomalies (curves, relative to 1961-90 means) of Northern California annual temperature (in ºC, above) and precipitation (in %, below) constructed by a sampling technique (Dettinger 2005) applied to an 84-member ensemble of IPCC 4th Assessment projections from 12 models responding to 3 GHG emission scenarios,. Symbols indicated 30-yr mean projected changes in various projections discussed here.

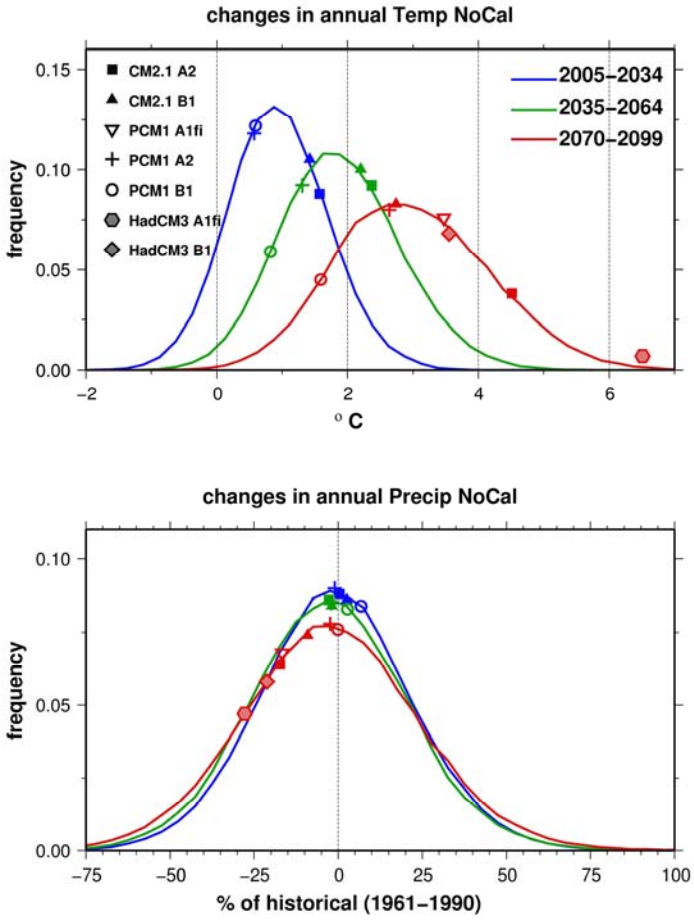

Figure 10. Joint probability distribution of annual temperature and precipitation anomalies, 2070-2099, relative to 1960-99 means, constructed from the IPCC4 ensemble described in caption of Fig. 9. P, G, and H designate 30-yr mean changes from PCM1, GFDL 2.1 and HadCM3 models; b, a, f designates B1, A2 and A1fi GHG scenarios.

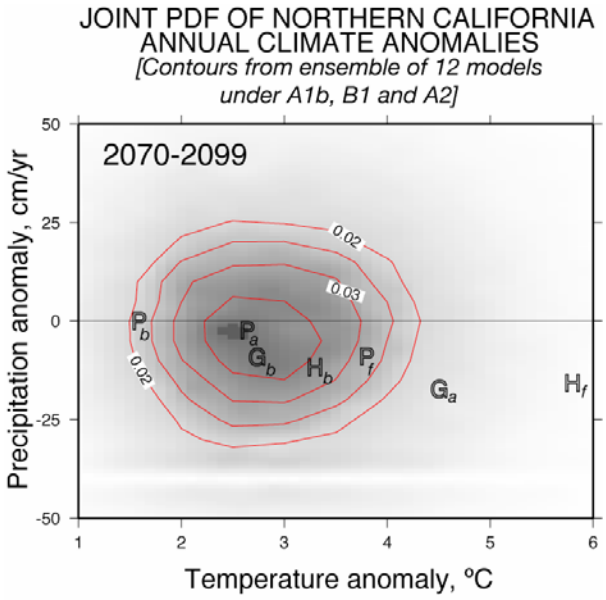

Figure 11. Time series of northern California temperature projections from 39 AR4 simulations with PCM (left) and GFDL (right), with the historical, B1 and A2 simulations analyzed here highlighted

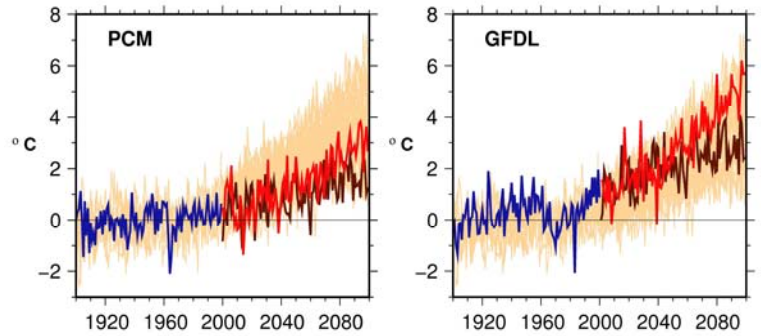

Figure 12. Distribution, binned by 1ºC intervals (percentages of total counts in the range from -10C to +10C), of daily northern California minimum temperatures (Tmin) for November-Marc1961-90 (blue) and 2070-99 (orange) on days that are dry, and on days with precipitation, from GFDL A2 (left) and PCM B1 (right) simulations.

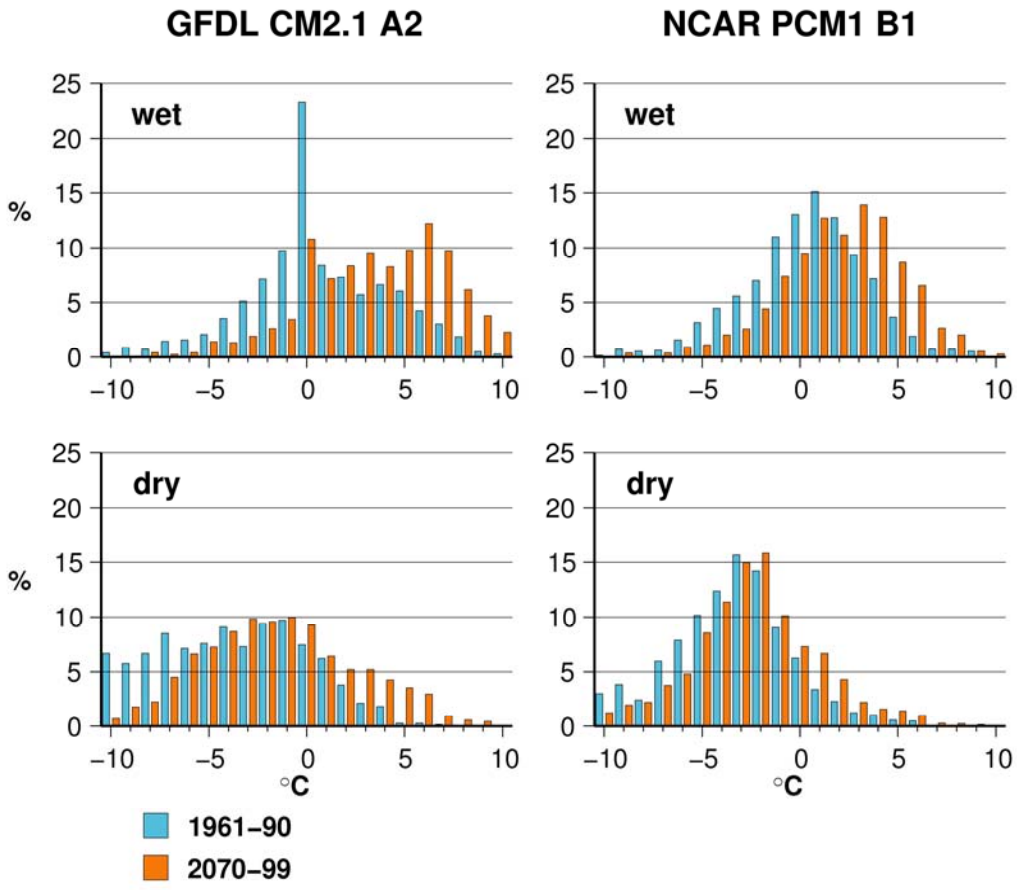

Figure 13. California statewide average April 1 snow water equivalents from 1961-90, 2005-2034, 2035-2064, and 2070-2099 simulations of PCM B1 and A2, and GFDL B1 and A2 conditions.

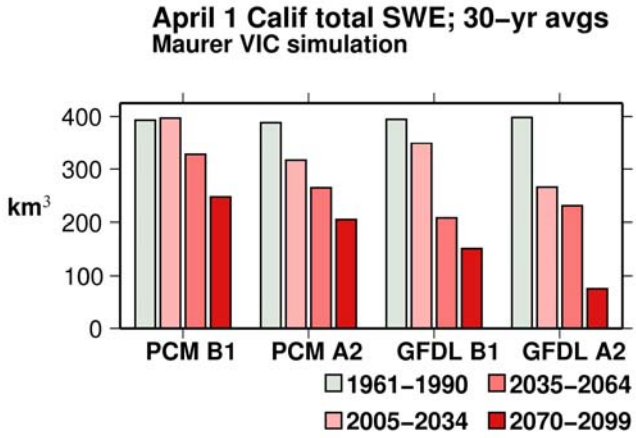

Figure 14. Change in springtime snow accumulation from the VIC hydrological model, driven by climate changes from GFDL A2 and PCM climate simulations. Changes are expressed as. ratio of 2070-2099 April 1 snow water equivalent (SWE) to historical (1961-1990).